Optimized Yolov8 to identify people with disabilities

Resty Wulanningrum [a,b,1], Anik Nur Handayani [a,2,*], Heru Wahyu Herwanto [a,3], Kohei Arai [c,4]

[a] Department of Electrical Engineering and Informatics, Faculty of Engineering, Universitas Negeri Malang, Malang, East Java, Indonesia
[b] Departement of Informatics Engineering, Universitas Nusantara PGRI Kediri, Kediri, East Java, Indonesia
[c] Department of Information Science, Saga University, Japan
[1] resty.wulanningrum.2305349@students.um.ac.id; [2] aniknur.ft@um.ac.id; [3] heru_wh@um.ac.id; [4] arai@cc.saga-u.ac.jp
* corresponding author

ARTICLE INFO

Article history
Received August 13, 2024
Revised October 17, 2024
Accepted February 6, 2025
Available online November 30, 2025

Selected paper from The 2024 7th International Symposium on Advanced Intelligent Informatics (SAIN'24), Nanjing, China, November 12-14, 2024, http://sain.ijain.org. Peer-reviewed by SAIN'24 Scientific Committee and Editorial Team of IJAIN journal.

Keywords
Optimized
Computer vision
Identify
Disabled
Yolov8

ABSTRACT

This research aims to develop an object detection model that can distinguish between the gait of people with and without disabilities with high accuracy. Object detection is currently designed to detect people and is used in both normal and gender-based gait recognition. Gait recognition, if further examined, encompasses recognition of both non-disabled and disabled individuals. Every day, people walk like most, but people with disabilities have different gaits from those of normal people. Some use walking aids, whereas others walk without them. YOLOv8 is a platform for detecting people. This research proposes an object detection for normal people and people with disabilities, both those who use assistive devices and those who do not. The dataset used is Disabled gait, comprising 6500 images, and will be divided into 3 data splits: 70% for training, 20% for validation, and 10% for testing. Model evaluation is based on precision, recall, mAP50, and mAP50-90. The test results for three classifications, namely assistive, non-assistive, and normal, show the highest value in the assistive class with an mAP50 value of 0.98 and an mAP50-95 value of 0.996. This study advances gait recognition by extending object detection to accurately differentiate normal and disabled walking patterns, including both assistive and non-assistive gaits, thereby enriching inclusive human-movement analysis. Beyond computer vision, the findings benefit healthcare, rehabilitation, and smart surveillance systems by enabling more accurate mobility assessment and accessibility-aware applications.

1. Introduction

Disability affects a person's mobility, which can affect how they walk [1], [2]. People with disabilities often experience difficulties or changes in how they move [4], [5], particularly with mobility [6], [7]. Gait recognition is a type of computer science research [8],[9] that studies how a person's legs and body move while walking [10]-[12]. This technology has been used for various purposes, such as surveillance [13],[14], security [15], and healthcare [16], [17]. There is considerable variation in the types and severity of gait impairment [18]. People with physical disabilities of the feet face style issues related to clothing choices that can affect their gait and overall quality of life [19]. Moreover, the use of wheelchairs or crutches to facilitate mobility is common among individuals with lower-limb impairments. This may result in physical difficulties, such as arthropathy, prolonged sitting, and hemoglobinopathies, which can impair a person's gait and overall health [20].

The impact of disability on gait performance is further highlighted by the fact that people with progressive multiple sclerosis (MS) also have altered gait patterns, which are characterized by decreased

cadence and speed when walking and increased muscle coactivation, particularly in difficult situations like decreased grip and increased cognitive load [21],[22]. Gait recognition in people with disabilities has important scientific, medical, social, and technological implications. It analyses a person's walking pattern to identify or monitor their physical condition, which is helpful for early detection of health problems such as Parkinson's or stroke. By detecting changes in gait earlier, medical personnel can intervene sooner, thereby speeding up a patient's recovery and helping to monitor the progress of rehabilitation.. The use of Deep Learning and Convolutional Neural Networks (CNNs) has resulted in impressive results in a variety of applications, including gait recognition [10], [23], [24], for more accurate and efficient feature extraction. These advancements in object recognition and gait identification technologies are recent [25].

You Only Look Once (YOLO) and, notably, its latest version, YOLOv8, offer significant improvements in speed, accuracy, and computational efficiency, making it well-suited for real-time applications [26], [27]. The YOLOv8 framework, developed in 2023, has undergone significant improvements over YOLOv7 and YOLOv5, resulting in improved efficiency and accuracy [28]-[31]. YOLOv8 is the latest object detection model, more accurate than previous versions, by adopting new techniques and optimizations [32]. The YOLO family of object detection and instance segmentation has grown rapidly over the past few years, with each new iteration introducing improvements in accuracy and/or speed [33].

This study offers several novel aspects: the application of YOLOv8 to disability gait identification [34], which combines sophisticated gait analysis with the power of object recognition [35] a multi-modal approach that uses visual data from videos converted into image frames to improve the accuracy of identification; the creation or use of custom datasets covering various disability types with and without assistive devices, allowing for more representative and accurate model training; and the optimization of models to operate on devices with limited computational resources.

In terms of technology, gait recognition plays a role in the development of advanced mobility devices [36], [37], such as prostheses with sensors that can adjust movements in real-time [38], [39], robotic exoskeletons [40]-[42], and smart wheelchairs [43]. These innovations can improve the comfort and independence of people with disabilities, allowing them to participate more actively in social and economic life by reducing dependence on others. Thus, it is essential to comprehend the connection between mobility and disability to comprehend the struggles of individuals with disabilities. Since the primary goal of this research is to identify people with disabilities based on their walking patterns, a thorough understanding of gait recognition is crucial to achieving its aims.

2. Method

This work comprises six stages: dataset collection, dataset splitting, training data, validation data, testing, and evaluation, as shown in Fig. 1.

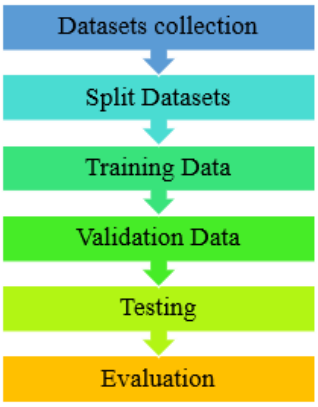

Fig. 1. Method for detection and segmentation

The dataset was obtained from DisabledGait [44] via Mendeley Data. This dataset was selected for its uniqueness, which includes individuals with disabilities who use assistive devices, individuals without assistive devices, and non-disabled individuals. In addition, this dataset has been annotated with instance segmentation annotations. Moreover, this dataset comprises a variety of backgrounds that reflect real-world conditions in the field and is not limited to a single background; it is divided into three classes: Assistive, Non-Assistive, and Normal. The data are already in image format, with labels for the three classes. The dataset comprises 6500 images and 130 videos, all of which are in image format. This dataset contains 6,500 images: 1,300 for the assistive class, 1,950 for the non-assistive class, and 3,250 for the normal class.

A dataset can be split into its three component parts: testing, validation, and training (as trained data). This is known as a split dataset. The features and patterns in the image will be recognized by the model. The model's parameters will be iteratively updated using the prediction error of the training data. Validation data is used to measure the model's performance during training in order to prevent overfitting and ensure that the trained model can learn from the training data as well as perform well on new data. After training is finished, testing data is utilized to assess the model's overall performance. This data is never used in the training or validation phases and is kept entirely separate. The final goal is to use previously unreviewed data to present an objective assessment of the model's performance.

YOLOv8 (You Only Look Once version 8) is known for its speed and efficiency [45], [46] in processing images in real-time with high accuracy [29], [32], which is critical in applications such as video surveillance in public places [47], security systems [48], and autonomous vehicles [49] that need to detect the presence of pedestrians quickly. Training data used the architecture of yolov8l with epoch [50] and image size 640x640 pixels [32]. Using 365 layers, 43632153 parameters, 43632137 gradients and 165.4 GFLOPs. Data validation using a custom model, namely by finding the best weights on the training data using 268 layers, 43608921 parameters, 0 gradients, and 164.8 GFLOPs.

Testing data with conf = 0.25 is used to determine whether a detection threshold is considered valid. In this study, detections with detection confidence below 0.25 are ignored. The results of model training on the YOLOv8 dataset include several metrics used for model evaluation, such as precision, recall, average precision, and mean Average Precision (mAP). Mean Average Precision (mAP) is a metric that measures the overall performance of an object detection model [27], [51], [52] by computing precision and recall across various prediction thresholds and then averaging them [53], [54], [55]. mAP at IoU 0.5 means that mAP is calculated with an IoU threshold of 0.5.

To calculate mAP at an IoU threshold of 0.5, the model first generates predicted bounding boxes for each image in the validation dataset; each prediction is associated with a confidence score and a class label, whereas the corresponding ground-truth bounding boxes are already defined. For each predicted bounding box, the Intersection over Union (IoU) with the corresponding ground-truth bounding box is computed using Equation (1) to quantify the degree of spatial overlap between the prediction and the reference annotation.

$$IoU = \frac{Area\ Of\ Intersection}{Area\ of\ Union} \tag{1}$$

After computing the IoU values, each prediction is categorized as a True Positive (TP), False Positive (FP), or False Negative (FN). A prediction is considered a True Positive if its IoU with the corresponding ground truth bounding box is at least 0.5 and the predicted class label is correct. A False Positive occurs when a predicted bounding box either has an IoU below 0.5 with any ground truth bounding box or is assigned an incorrect class label. Conversely, a False Negative refers to a ground-truth bounding box that the model fails to detect, indicated by the absence of a corresponding prediction with IoU ≥ 0.5. Based on these classifications, precision and recall are calculated, where precision is defined as the proportion of True Positives relative to the total number of predicted positives, expressed as TP/(TP + FP), as shown in Equation (2).

$$Precision = \frac{TP}{TP+FP} \quad (2)$$

Recall is defined as the proportion of True Positives relative to the total number of actual positives, measuring the model's ability to correctly detect relevant objects. It is calculated as the ratio of TP to the sum of TP and FN, as expressed in Equation (3).

$$Recall = \frac{TP}{TP+FN} \quad (3)$$

To further evaluate detection performance, a precision–recall curve is constructed by varying the prediction confidence threshold from 0 to 1 and computing the corresponding precision and recall values at each threshold. The Average Precision (AP) for each object class is then calculated as the area under its precision–recall curve, which summarizes detection performance across all confidence levels. Finally, the Mean Average Precision (mAP) is computed as the average of AP across all object classes, providing an overall performance metric for the detection model, as defined in Equation (4).

$$mAP = \frac{1}{2} \sum_{i=1}^{N} AP_i \quad (4)$$

where N is the number of object classes.

3. Results and Discussion

3.1. Dataset Collection

We used a publicly available dataset, DisabledGait, available on Mendeley Data, which contains 6500 labelled images. The annotation folder contains two files: train and data.yaml. The train folder has two subfolders, images and labels. The images subfolder contains 6500 images, and the labels subfolder contains labels corresponding to those images. This structure is shown in Fig. 2.

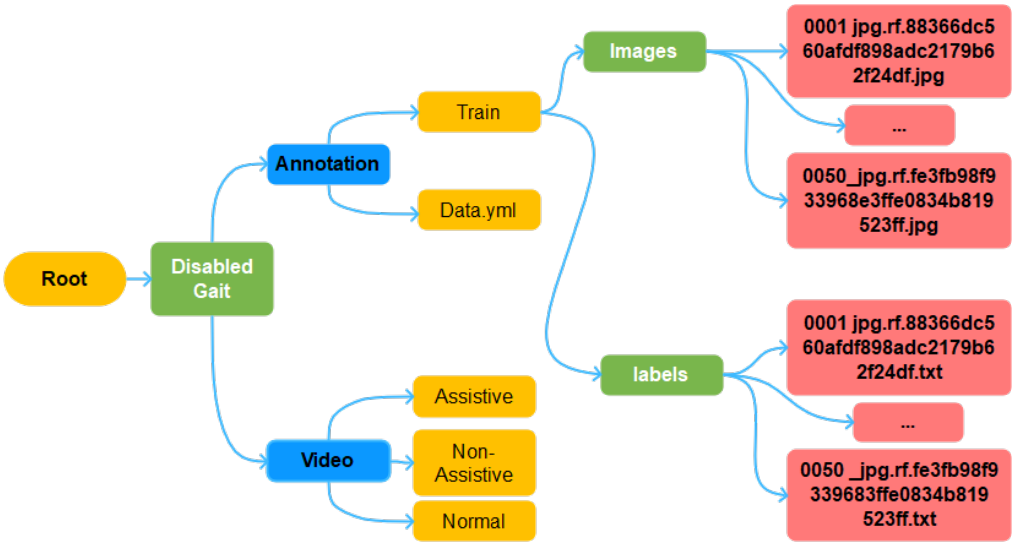

Fig. 2. Structure dataset

3.2. Split Dataset

Splitting data is an essential step in preparing a dataset for machine learning and statistical analysis. It involves dividing the dataset into training, validation, and test subsets to train, validate, and evaluate models, ensuring that performance is evaluated fairly and helping to prevent overfitting. The training set, comprising 70% of the total dataset (4550 data points), is used to train the model so that it can learn patterns and relationships. The validation set, which is 20% of the dataset (1300 data points), is used to tune hyperparameters and evaluate model performance during training, aiding in model selection and providing an unbiased evaluation of model fit. Finally, the test set, comprising 10% of the dataset

(650 data points), is used to assess the model's performance after training, providing an unbiased evaluation. Importantly, the test set should not be used during the training or validation process to ensure an accurate measure of the model's ability to generalize to new data.

3.3. Training Data

Training data results will be stored inc table form which contains epoch, train/box_loss, train/cls_loss, train/dfl_loss, metrics/precision(B), metrics/recall(B), metrics/mAP50(B), metrics/mAP50-95(B), val/box_loss, val/cls_loss, val/dfl_loss, Ir/pg0, Ir/pg1, Ir/pg2, show in Fig. 3.

	epoch,	train/box_loss,	train/cls_loss,	train/dfl_loss,	metrics/precision(B),	metrics/recall(B),	metrics/mAP50(B),	metrics/mAP50-95(B),	val/box_loss,	val/cls_loss,	val/dfl_loss,	Ir/pg0,	Ir/pg1,	Ir/pg2
2	0	0.57961,	10.556,00	0.9915,	0.98494,	0.96233,	0.96537,	0.88376,	0.40372,	0.25158,	0.89519,	0.07011,	0.0033211,	0.0033211
3	1	0.56208,	0.47705,	0.96885,	0.9923,	0.96061,	0.96189,	0.86961,	0.43978,	0.34074,	0.92875,	0.039979,	0.0065227,	0.0065227
4	2	0.65832,	0.56945,	10.184,00	0.99212,	0.9594,	0.96108,	0.83245,	0.50794,	0.39983,	0.99834,	0.0097148,	0.0095922,	0.0095922
5	3	0.72643,	0.62764,	10.619,00	0.91323,	0.90541,	0.94987,	0.81741,	0.55497,	0.47727,	10.421,00	0.009406,	0.009406,	0.009406
6	4	0.72656,	0.60331,	10.656,00	0.97277,	0.94623,	0.95874,	0.84481,	0.50512,	0.60514,	0.98792,	0.009406,	0.009406,	0.009406
7	5	0.68731,	0.56468,	10.465,00	0.98246,	0.95401,	0.9603,	0.8423,	0.50717,	0.41941,	10.002,00	0.009208,	0.009208,	0.009208
8	6	0.67573,	0.53508,	10.348,00	0.99663,	0.96319,	0.96585,	0.8838,	0.42668,	0.29773,	0.93415,	0.00901,	0.00901,	0.00901
9	7	0.65198,	0.51547,	10.275,00	0.99392,	0.96163,	0.9615,	0.87862,	0.42242,	0.30956,	0.91736,	0.008812,	0.008812,	0.008812
10	8	0.62184,	0.48358,	10.107,00	0.99656,	0.96292,	0.9634,	0.88514,	0.40891,	0.2904,	0.89741,	0.008614,	0.008614,	0.008614
11	9	0.61924,	0.47629,	10.112,00	0.98036,	0.95688,	0.96126,	0.87762,	0.40815,	0.30107,	0.91624,	0.008416,	0.008416,	0.008416
12	10	0.60646,	0.46315,	10.018,00	0.99674,	0.96308,	0.96345,	0.89055,	0.38282,	0.26164,	0.90269,	0.008218,	0.008218,	0.008218
13	11	0.58917,	0.44467,	0.99707,	0.99669,	0.96273,	0.96556,	0.90548,	0.35987,	0.24356,	0.89204,	0.00802,	0.00802,	0.00802
14	12	0.57355,	0.42833,	0.98579,	0.99627,	0.96319,	0.96592,	0.90504,	0.34981,	0.25777,	0.87865,	0.007822,	0.007822,	0.007822
15	13	0.5713,	0.42077,	0.98585,	0.99653,	0.96006,	0.96899,	0.91409,	0.34821,	0.23589,	0.88583,	0.007624,	0.007624,	0.007624
16	14	0.55277,	0.40029,	0.97631,	0.99666,	0.96319,	0.96783,	0.91175,	0.34349,	0.22593,	0.88474,	0.007426,	0.007426,	0.007426
17	15	0.54389,	0.40051,	0.97207,	0.99695,	0.96319,	0.96689,	0.91339,	0.35003,	0.23947,	0.87898,	0.007228,	0.007228,	0.007228
18	16	0.53767,	0.39499,	0.97169,	0.9966,	0.96319,	0.96757,	0.91697,	0.33691,	0.22179,	0.87316,	0.00703,	0.00703,	0.00703
19	17	0.53431,	0.38979,	0.971,	0.99697,	0.96319,	0.96539,	0.92038,	0.32496,	0.22062,	0.86797,	0.006832,	0.006832,	0.006832
20	18	0.52654,	0.38249,	0.96493,	0.99616,	0.96319,	0.96756,	0.92575,	0.32178,	0.21798,	0.88332,	0.006634,	0.006634,	0.006634
21	19	0.51622,	0.37145,	0.964,	0.99702,	0.96319,	0.96999,	0.92666,	0.32364,	0.20737,	0.86366,	0.006436,	0.006436,	0.006436
22	20	0.51116,	0.36667,	0.95874,	0.99684,	0.96319,	0.96901,	0.91925,	0.31857,	0.20616,	0.86279,	0.006238,	0.006238,	0.006238
23	21	0.51024,	0.35696,	0.94908,	0.9969,	0.96319,	0.96836,	0.933,	0.30417,	0.19222,	0.84854,	0.00604,	0.00604,	0.00604
24	22	0.49967,	0.35437,	0.95356,	0.99668,	0.96319,	0.96733,	0.93038,	0.30548,	0.19632,	0.85699,	0.005842,	0.005842,	0.005842
25	23	0.4988,	0.34799,	0.9441,	0.99695,	0.96319,	0.96995,	0.9358,	0.29778,	0.19265,	0.84992,	0.005644,	0.005644,	0.005644

Fig. 3. Example of Training Result for 24 first rows

As shown in Fig. 4, this study identified and visualized three gait-related classes via bounding box detection: the assistive code group labeled 0, the non-assistive code group labeled 1, and the normal code group labeled 2. The figure illustrates that the proposed YOLOv8-based model can detect individuals under diverse environmental conditions, camera angles, and backgrounds, while simultaneously distinguishing gait characteristics associated with the use of assistive devices, atypical but non-assistive walking patterns, and normal gait. The bounding boxes and class labels demonstrate that the model consistently localizes subjects and assigns the correct class, highlighting its robustness to real-world gait variability and supporting its effectiveness for inclusive gait recognition tasks.

Fig. 4. Train Batch 0

The machine learning model's performance graph for identifying objects linked to disabled and non-disabled people is shown in Fig. 5. The y-axis displays performance metrics like mean average precision (mAP), recall, loss, and precision, and the x-axis represents the number of epochs, or full cycles of processing all training data. The graph shows effective model training, as evidenced by rising precision, recall, and mAP, alongside falling loss. Furthermore, the box_loss value, a measure of the prediction accuracy between the item and the bounding box, is compared between the training and validation results. In the fifth epoch, the training box_loss reached its maximum at 0.72656 and decreased to 0.25188, whereas in the fourth epoch, the validation box_loss reached its maximum at 0.55497 and decreased to 0.24023 in the 50th epoch. The distribution for the bounding box of the picture object is predicted using distribution focal loss, or DFL. The lowest value, 0.84059, occurs at the 50th epoch, and the highest value, 1.0656, occurs at the 5th epoch, for the validation dfl_loss. Lower values of validation box_loss, cls_loss, and dfl_loss show good generalization to unobserved data, prevent overfitting, and enable more precise bounding box prediction.

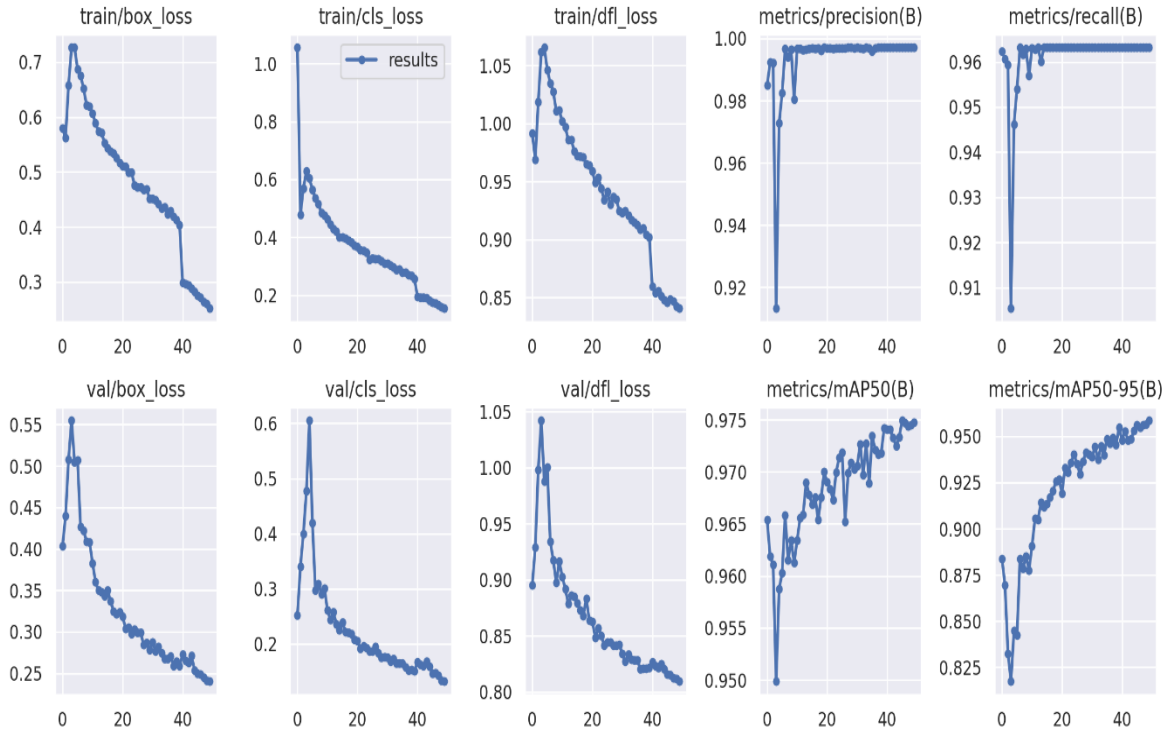

Fig. 5. Machine learning model's performance graph for identifying objects

3.4. Validation Data

Data validation involves two models: label validation and prediction validation. Label validation ensures that data labels are correct and consistent, which is crucial for supervised learning tasks in which the model learns from labeled data. Predict validation, on the other hand, involves verifying the model's predictions against a held-out validation set to assess its accuracy and generalization. This process helps identify overfitting and underfitting, enabling adjustments to improve model performance.

Fig. 6 presents the results of label validation, demonstrating the correctness and consistency of the ground-truth annotations used in this study. As shown in the figure, each validation image is accurately labeled into one of the three predefined classes, assistive, non-assistive, and normal, with bounding boxes tightly enclosing the subjects and class labels correctly reflecting their gait characteristics. This validation step confirms that the dataset annotations are reliable and free from class ambiguity, which is essential for effective supervised learning. By ensuring that labels accurately reflect real gait conditions during model training and evaluation, label validation reduces the risk of biased learning. It supports more accurate performance assessment in the subsequent prediction-validation stage.

Fig. 6. Validation label

Fig. 7 illustrates the validation results, in which the trained YOLOv8 model's outputs are evaluated on the validation dataset to assess detection accuracy and generalization capability. As shown in the figure, the model successfully predicts the three gait classes, assistive, non-assistive, and normal, with high confidence scores, indicating strong agreement between predicted labels and the validated ground truth. The bounding boxes are consistently well-aligned with the subjects, demonstrating accurate localization, while the predicted class labels reflect the underlying gait characteristics across varied environments and walking conditions. This validation process is essential for identifying potential overfitting or underfitting, as it reveals how well the model performs on unseen data and confirms that the proposed approach generalizes effectively beyond the training set.

Fig. 7. Validation Predict

3.5. Testing

Testing object detection is an important step in the development and evaluation process of object recognition systems. This process involves using various datasets to test the model's ability to identify and classify objects with high accuracy. Testing is done by comparing the model's output against ground

truth data, which is data that has been manually labelled and is considered a true reference, to show how well the model can detect objects under various conditions such as different lighting, diverse viewing angles, and complex backgrounds. In addition, testing aims to identify the shortcomings and weaknesses of the object detection model. Analysis of the test results allows researchers to identify areas where the model has difficulty, such as in recognizing overlapping objects or in situations with high noise. This information is crucial for model improvement and refinement, so comprehensive and repeated testing enables researchers to optimize model performance and achieve high levels of accuracy and reliability in real applications.

Fig. 8 is the result of the system test. In the normal person label, it has a confidence score of 0.95, and assistive has a confidence score of 0.96 and non-assistive has a confidence score of 0.95. The scale in confidence score is 0 to 1, and the closer the confidence score is to 1, the higher the confidence of the model that the classification is correct

Fig. 8. Test Result

3.6. Evaluation

Model evaluation is the process of assessing the performance of a machine learning or statistical model using certain metrics to determine how well the model performs on data not seen during training. The results of the model evaluation are shown in the Table 1.

Table 1. Evaluation

Class	P	R	mAP50	mAP50-95
All	0.997	0.963	0.975	0.958
Assistive	0.996	0.977	0.98	0.966
Non-Assistive	0.997	0.956	0.97	0.947
Normal	0.998	0.956	0.974	0.962

Model Performance is Generally Good: Precision, Recall, and mAP values for all classes are quite high, close to 1. This indicates that the model generally detects objects with high accuracy. Best Performance for "Assistive" Class: The "Assistive" class achieves the highest mAP of 0.98, indicating that the model is best at detecting objects in this class. Lowest Performance for the "Normal" Class: The "Normal" class has a slightly lower mAP of 0.974 than the other classes, indicating that the model may be somewhat less accurate at detecting objects from this class. The "Non-Assistive" class has an mAP of 0.97. The object detection models evaluated in this Table demonstrate excellent performance across various object classes.

4. Conclusion

In this research, we propose an innovative model for disabled gait recognition using YOLOv8. This model improves detection performance for both healthy and disabled individuals by using the DisabledGait database. Based on the results and discussion presented, this research draws several

conclusions. First, YOLOv8 is capable of detecting normal people, assistive people with disabilities, and non-assistive people without disabilities. Second, the image processing module used for training, validation, and data testing is able to effectively acquire and utilize image information, resulting in high confidence score values. Third, the evaluation results showed that the assistive class had the highest mAP value of 0.98, while the non-assistive class had the lowest mAP value of 0.97. This may be due to the standing position of people with non-assistive disabilities who are still able to stand upright, causing errors in detection. Future research can add segmentation models to improve object detection. The use of segmentation will provide more detail in object recognition, especially since the data has varied backgrounds. It is expected that the addition of segmentation will improve the performance and accuracy of the system in recognizing individuals with disabilities who use assistive devices, without assistive devices, and normal people. In the future, this technology is expected to be applied to real-time cameras to help priorities public services for individuals with disabilities.

Declarations

Author contribution. Resty Wulanningrum: Writing original draft, Software, Visualization, Resource, data curation. Anik Nur Handayani: Supervision, project administration, formal analysis, review & editing draft, validation. Heru Wahyu Herwanto: Conceptualization, resources, methodology, conceptualization, proofreading.
Funding statement. None of the authors have received any funding or grants from any institution or funding body for the research.
Conflict of interest. The authors declare no conflict of interest.
Additional information. No additional information is available for this paper.

References

[1] R. Bennett and R. Vijaygopal, "Exploring mobility and transportation technology futures for people with ambulatory disabilities: A science fiction prototype," *Technovation*, vol. 133, p. 103001, 2024, doi: 10.1016/j.technovation.2024.103001.

[2] M. Yang, S. Fraser, and T. O'Sullivan, "'I've already lived like There's a pandemic': A grounded theory study on the experiences of people with a mobility disability," *International Journal of Disaster Risk Reduction*, vol. 99, p. 104116, 2023, doi: 10.1016/j.ijdrr.2023.104116.

[3] A. Neven and W. Ectors, "'I am dependent on others to get there': Mobility barriers and solutions for societal participation by persons with disabilities," *Travel Behav Soc*, vol. 30, pp. 302–311, 2023, doi: 10.1016/j.tbs.2022.10.009.

[4] M. Yang, S. Fraser, and T. O'Sullivan, "'I've already lived like There's a pandemic': A grounded theory study on the experiences of people with a mobility disability," *International Journal of Disaster Risk Reduction*, vol. 99, p. 104116, 2023, doi: 10.1016/j.ijdrr.2023.104116.

[5] S. Demiröz Yıldırım, "Integrated disaster management experience of people with disabilities: A phenomenological research on the experience of people with orthopedic disabilities in Türkiye," *International Journal of Disaster Risk Reduction*, vol. 88, p. 103611, 2023, doi: 10.1016/j.ijdrr.2023.103611.

[6] C. L. A. Wender *et al.*, "Rationale and methodology for examining the combination of aerobic exercise and cognitive rehabilitation on new learning and memory in persons with multiple sclerosis and mobility disability: Protocol for a randomized controlled trial," *Contemp Clin Trials*, vol. 144, p. 107630, 2024, doi: 10.1016/j.cct.2024.107630.

[7] J. Heo *et al.*, "A framework of transportation mode detection for people with mobility disability," *J Intell Transp Syst*, 2024, doi: 10.1080/15472450.2024.2329901.

[8] L. Hu *et al.*, "Application of gaming robot based on gait recognition algorithm in sports training and assistance system," *Entertain Comput*, vol. 52, p. 100763, 2025, doi: 10.1016/j.entcom.2024.100763.

[9] X. Liu, Q. Li, S. Hou, M. Ren, X. Hu, and Y. Huang, "Depression risk recognition based on gait: A benchmark," *Neurocomputing*, vol. 596, p. 128045, 2024, doi: 10.1016/j.neucom.2024.128045.

[10] B. Ali, M. Bukhari, M. Maqsood, J. Moon, E. Hwang, and S. Rho, "An end-to-end gait recognition system for covariate conditions using custom kernel CNN," *Heliyon*, vol. 10, no. 12, p. e32934, 2024, doi: 10.1016/j.heliyon.2024.e32934.

[11] S. M. H. Sithi Shameem Fathima, K. A. Jyotsna, T. Srinivasulu, K. Archana, M. Tulasi rama, and S. Ravichand, "Walking pattern analysis using GAIT cycles and silhouettes for clinical applications," *Measurement: Sensors*, vol. 30, p. 100893, 2023, doi: 10.1016/j.measen.2023.100893.

[12] Y. Liu, X. Liu, Z. Wang, X. Yang, and X. Wang, "Improving performance of human action intent recognition: Analysis of gait recognition machine learning algorithms and optimal combination with inertial measurement units," *Comput Biol Med*, vol. 163, p. 107192, 2023, doi: 10.1016/j.compbiomed.2023.107192.

[13] A. Parashar, A. Parashar, A. F. Abate, R. S. Shekhawat, and I. Rida, "Real-time gait biometrics for surveillance applications: A review," *Image Vis Comput*, vol. 138, p. 104784, 2023, doi: 10.1016/j.imavis.2023.104784.

[14] Y. Liu, C. Wang, H. Li, and Y. Zhou, "Gait recognition of camouflaged people based on UAV infrared imaging," *Infrared Phys Technol*, vol. 138, p. 105262, 2024, doi: 10.1016/j.infrared.2024.105262.

[15] Z. He, W. Wang, J. Dong, and T. Tan, "Temporal sparse adversarial attack on sequence-based gait recognition," *Pattern Recognit*, vol. 133, p. 109028, 2023, doi: 10.1016/j.patcog.2022.109028.

[16] X. Liu, Q. Li, S. Hou, M. Ren, X. Hu, and Y. Huang, "Depression risk recognition based on gait: A benchmark," *Neurocomputing*, vol. 596, p. 128045, 2024, doi: 10.1016/j.neucom.2024.128045.

[17] D. Guo *et al.*, "Degradable, biocompatible, and flexible capacitive pressure sensor for intelligent gait recognition and rehabilitation training," *Nano Energy*, vol. 127, p. 109750, 2024, doi: 10.1016/j.nanoen.2024.109750.

[18] T. Zanotto *et al.*, "Variability of objective gait measures across the expanded disability status scale in people living with multiple sclerosis: A cross-sectional retrospective analysis," *Mult Scler Relat Disord*, vol. 59, p. 103645, 2022, doi: 10.1016/j.msard.2022.103645.

[19] T. N. Bryce, Huang Vincent, and M. X. Escalon, "49 - Spinal Cord Injury," in *Braddom's Physical Medicine and Rehabilitation (Sixth Edition)*, D. X. Cifu, Ed., Philadelphia: Elsevier, 2021, pp. 1049-1100.e6. doi: 10.1016/B978-0-323-62539-5.00049-7.

[20] Y. MORI, K. E. N. MAEJIMA, K. INOUE, N. SHIROMA, and Y. FUKUOKA, "ABLE: A STANDING STYLE TRANSFER SYSTEM FOR A PERSON WITH DISABLED LOWER LIMBS," in *Emerging Trends in Mobile Robotics*, WORLD SCIENTIFIC, 2010, pp. 1071–1078. doi: 10.1142/9789814329927_0131.

[21] M. Pau *et al.*, "Inter-joint coordination during gait in people with multiple sclerosis: A focus on the effect of disability," *Mult Scler Relat Disord*, vol. 60, p. 103741, 2022, doi: 10.1016/j.msard.2022.103741.

[22] S.-C. Huang *et al.*, "The Danger of Walking with Socks: Evidence from Kinematic Analysis in People with Progressive Multiple Sclerosis," *Sensors*, vol. 20, no. 21, 2020, doi: 10.3390/s20216160.

[23] L. Qin, M. Guo, K. Zhou, X. Chen, and J. Qiu, "Gait recognition using deep learning with handling defective data from multiple wearable sensors," *Digit Signal Process*, vol. 154, p. 104665, 2024, doi: 10.1016/j.dsp.2024.104665.

[24] R. A. Asmara *et al.*, "Comparative Study of Gait Gender Identification using Gait Energy Image (GEI) and Gait Information Image (GII)," in *MATEC Web of Conferences*, EDP Sciences, Sep. 2018. doi: 10.1051/matecconf/201819715006.

[25] A. Parashar, A. Parashar, M. Shabaz, D. Gupta, A. K. Sahu, and M. A. Khan, "Advancements in artificial intelligence for biometrics: A deep dive into model-based gait recognition techniques," *Eng Appl Artif Intell*, vol. 130, p. 107712, 2024, doi: 10.1016/j.engappai.2023.107712.

[26] J. Mao, L. Wang, N. Wang, Y. Hu, and W. Sheng, "A novel method of human identification based on dental impression image," *Pattern Recognit*, vol. 144, p. 109864, 2023, doi: 10.1016/j.patcog.2023.109864.

[27] R. A. Asmara, B. Syahputro, D. Supriyanto, and A. N. Handayani, "Prediction of traffic density using yolo object detection and implemented in raspberry pi 3b + and intel ncs 2," in *4th International Conference on*

Vocational Education and Training, ICOVET 2020, Institute of Electrical and Electronics Engineers Inc., Sep. 2020, pp. 391–395. doi: 10.1109/ICOVET50258.2020.9230145.

[28] R. Sapkota, D. Ahmed, and M. Karkee, "Comparing YOLOv8 and Mask R-CNN for instance segmentation in complex orchard environments," *Artificial Intelligence in Agriculture*, 2024, doi: 10.1016/j.aiia.2024.07.001.

[29] J. Terven and D. Cordova-Esparza, "A Comprehensive Review of YOLO Architectures in Computer Vision: From YOLOv1 to YOLOv8 and YOLO-NAS," Apr. 2023, doi: 10.3390/make5040083.

[30] A. Aboah, B. Wang, U. Bagci, and Y. Adu-Gyamfi, "Real-time Multi-Class Helmet Violation Detection Using Few-Shot Data Sampling Technique and YOLOv8," Apr. 2023, [Online]. Available: http://arxiv.org/abs/2304.08256

[31] Y. Zhang, Y. Lu, W. Zhu, X. Wei, and Z. Wei, "Traffic sign detection based on multi-scale feature extraction and cascade feature fusion," *J Supercomput*, vol. 79, no. 2, pp. 2137–2152, 2023, doi: 10.1007/s11227-022-04670-6.

[32] C. Zhang, X. Chen, P. Liu, B. He, W. Li, and T. Song, "Automated detection and segmentation of tunnel defects and objects using YOLOv8-CM," *Tunnelling and Underground Space Technology*, vol. 150, p. 105857, 2024, doi: 10.1016/j.tust.2024.105857.

[33] R. Sapkota, D. Ahmed, and M. Karkee, "Comparing YOLOv8 and Mask R-CNN for instance segmentation in complex orchard environments," *Artificial Intelligence in Agriculture*, vol. 13, pp. 84–99, 2024, doi: 10.1016/j.aiia.2024.07.001.

[34] T. Zanotto *et al.*, "Variability of objective gait measures across the expanded disability status scale in people living with multiple sclerosis: A cross-sectional retrospective analysis," *Mult Scler Relat Disord*, vol. 59, p. 103645, 2022, doi: 10.1016/j.msard.2022.103645.

[35] M. H. Khan, M. S. Farid, and M. Grzegorzek, "Vision-based approaches towards person identification using gait," *Comput Sci Rev*, vol. 42, p. 100432, 2021, doi: 10.1016/j.cosrev.2021.100432.

[36] D. Xu *et al.*, "A new method proposed for realizing human gait pattern recognition: Inspirations for the application of sports and clinical gait analysis," *Gait Posture*, vol. 107, pp. 293–305, 2024, doi: 10.1016/j.gaitpost.2023.10.019.

[37] D. Zhang, Z. Xu, Z. Wang, H. Cai, J. Wang, and K. Li, "Machine-learning-assisted wearable PVA/Acrylic fluorescent layer-based triboelectric sensor for motion, gait and individual recognition," *Chemical Engineering Journal*, vol. 478, p. 147075, 2023, doi: 10.1016/j.cej.2023.147075.

[38] S. Manz, D. Seifert, B. Altenburg, T. Schmalz, S. Dosen, and J. Gonzalez-Vargas, "Using embedded prosthesis sensors for clinical gait analyses in people with lower limb amputation: A feasibility study," *Clinical Biomechanics*, vol. 106, p. 105988, 2023, doi: 10.1016/j.clinbiomech.2023.105988.

[39] S. Kansal, D. Garg, A. Upadhyay, S. Mittal, and G. S. Talwar, "DL-AMPUT-EEG: Design and development of the low-cost prosthesis for rehabilitation of upper limb amputees using deep-learning-based techniques," *Eng Appl Artif Intell*, vol. 126, p. 106990, 2023, doi: 10.1016/j.engappai.2023.106990.

[40] H. Yu, A. Nelson, Z. Huang, and M. S. Erden, "Purpose-centered design of rehabilitation robots: a case study of a hand exoskeleton for assessing spasticity," *Procedia CIRP*, vol. 128, pp. 227–232, 2024, doi: 10.1016/j.procir.2024.06.019.

[41] A. Q. AL-DUJAILI, A. F. Hasan, A. J. Humaidi, and A. Al-Jodah, "Anti-disturbance control design of Exoskeleton Knee robotic system for rehabilitative care," *Heliyon*, vol. 10, no. 9, p. e28911, 2024, doi: 10.1016/j.heliyon.2024.e28911.

[42] A. Ghaffar *et al.*, "Efficiency, optimality, and selection in a rigid actuation system with matching capabilities for an assistive robotic exoskeleton," *Engineering Science and Technology, an International Journal*, vol. 51, p. 101613, 2024, doi: 10.1016/j.jestch.2023.101613.

[43] F. Utaminingrum, A. W. S. B. Johan, I. K. Somawirata, T. K. Shih, and C.-Y. Lin, "Indoor staircase detection for supporting security systems in autonomous smart wheelchairs based on deep analysis of the Co-occurrence Matrix and Binary Classification," *Intelligent Systems with Applications*, vol. 23, p. 200405, 2024, doi: 10.1016/j.iswa.2024.200405.

[44] R. Wulanningrum, A. N. Handayani, and H. W. Herwanto, "DissabledGait: Gait Dataset of Normal People and People with Disabilities," Mendeley Data. Accessed: May 25, 2024. [Online]. Available: https://data.mendeley.com/datasets/v6hy35ydch/1

[45] L. Zhao *et al.*, "YOLOv8-QR: An improved YOLOv8 model via attention mechanism for object detection of QR code defects," *Computers and Electrical Engineering*, vol. 118, p. 109376, 2024, doi: 10.1016/j.compeleceng.2024.109376.

[46] R. A. Asmara *et al.*, "YOLO-based object detection performance evaluation for automatic target aimbot in first-person shooter games," *Bulletin of Electrical Engineering and Informatics*, vol. 13, no. 4, pp. 2456–2470, Aug. 2024, doi: 10.11591/eei.v13i4.6895.

[47] M. Bakirci, "Enhancing vehicle detection in intelligent transportation systems via autonomous UAV platform and YOLOv8 integration," *Appl Soft Comput*, vol. 164, p. 112015, 2024, doi: 10.1016/j.asoc.2024.112015.

[48] M. Bakirci, "Utilizing YOLOv8 for enhanced traffic monitoring in intelligent transportation systems (ITS) applications," *Digit Signal Process*, vol. 152, p. 104594, 2024, doi: 10.1016/j.dsp.2024.104594.

[49] S. Sun, B. Mo, J. Xu, D. Li, J. Zhao, and S. Han, "Multi-YOLOv8: An infrared moving small object detection model based on YOLOv8 for air vehicle," *Neurocomputing*, vol. 588, p. 127685, 2024, doi: 10.1016/j.neucom.2024.127685.

[50] H. Min *et al.*, "Automatic classification of distal radius fracture using a two-stage ensemble deep learning framework," *Phys Eng Sci Med*, vol. 46, no. 2, pp. 877–886, Jun. 2023, doi: 10.1007/s13246-023-01261-4.

[51] C.-J. Zhang *et al.*, "Evaluation of the YOLO models for discrimination of the alfalfa pollinating bee species," *J Asia Pac Entomol*, vol. 27, no. 1, p. 102195, 2024, doi: 10.1016/j.aspen.2023.102195.

[52] Q. Li, W. Ma, H. Li, X. Zhang, R. Zhang, and W. Zhou, "Cotton-YOLO: Improved YOLOV7 for rapid detection of foreign fibers in seed cotton," *Comput Electron Agric*, vol. 219, p. 108752, 2024, doi: 10.1016/j.compag.2024.108752.

[53] Y. Peng *et al.*, "A dynamic individual method for yak heifer live body weight estimation using the YOLOv8 network and body parameter detection algorithm," *J Dairy Sci*, vol. 107, no. 8, pp. 6178–6191, 2024, doi: 10.3168/jds.2023-24065.

[54] C. Xiong, T. Zayed, and E. M. Abdelkader, "A novel YOLOv8-GAM-Wise-IoU model for automated detection of bridge surface cracks," *Constr Build Mater*, vol. 414, p. 135025, 2024, doi: 10.1016/j.conbuildmat.2024.135025.

[55] R. A. Asmara *et al.*, "YOLO-based object detection performance evaluation for automatic target aimbot in first-person shooter games," *Bulletin of Electrical Engineering and Informatics*, vol. 13, no. 4, pp. 2456–2470, Aug. 2024, doi: 10.11591/eei.v13i4.6895.